© 2016. Published by The Company of Biologists Ltd | Journal of Experimental Biology (2016) 219, 1833-1842 doi:10.1242/jeb.138859

RESEARCH ARTICLE

The extraordinary joint material of an articulated coralline alga. I. Mechanical characterization of a key adaptation

Mark W. Denny* and Felicia A. King

ABSTRACT

Flexibility is key to survival for seaweeds exposed to the extreme hydrodynamic environment of wave-washed rocky shores. This poses a problem for coralline algae, whose calcified cell walls make them rigid. Through the course of evolution, erect coralline algae have solved this problem by incorporating joints (genicula) into their morphology, allowing their fronds to be as flexible as those of uncalcified seaweeds. To provide the flexibility required by this structural innovation, the joint material of *Calliarthron cheilosporioides*, a representative articulated coralline alga, relies on an extraordinary tissue that is stronger, more extensible and more fatigue resistant than the tissue of other algal fronds. Here, we report on experiments that reveal the viscoelastic properties of this material. On the one hand, its compliance is independent of the rate of deformation across a wide range of deformation rates, a characteristic of elastic solids. This deformation rate independence allows joints to maintain their flexibility when loaded by the unpredictable – and often rapidly imposed – hydrodynamic force of breaking waves. On the other hand, the genicular material has viscous characteristics that similarly augment its function. The genicular material dissipates much of the energy absorbed as a joint is deformed during cyclic wave loading, which potentially reduces the chance of failure by fatigue, and the material accrues a limited amount of deformation through time. This limited creep increases the flexibility of the joints while preventing them from gradually stretching to the point of failure. These new findings provide the basis for understanding how the microscale architecture of genicular cell walls results in the adaptive mechanical properties of coralline algal joints.

KEY WORDS: Flexibility, *Calliarthron cheilosporioides*, Material properties, Viscoelasticity, Creep, Stress relaxation, Stress recovery, Ecological mechanics

INTRODUCTION

The seaweeds of wave-swept rocky shores inhabit one of the most physically stressful environments on Earth. For example, when the tide is in, intertidal seaweeds must cope with the hydrodynamic forces imposed by breaking waves, in which water velocities can exceed 20 m s^{-1} (Denny, 1988; Gaylord, 1999; Denny et al., 2003). Despite this physical challenge, wave-washed shores support a notably diverse set of macroalgae, and this unusual occurrence of diversity in the face of adversity uniquely sets the stage for comparative studies of algal functional morphology. Previous research on the mechanical characteristics of seaweeds has shown that flexibility is the design criterion that best accounts for their ability to withstand hydrodynamic forces (Koehl, 1984, 1986; Harder et al., 2004). A function of both shape and material properties, flexibility allows seaweeds to assume more streamlined shapes and 'go with the flow', which reduces the drag imposed by waves (e.g. Denny and Gaylord, 2002; Boller and Carrington, 2006; Martone et al., 2012).

Articulated, erect coralline red algae provide an exceptional opportunity to evaluate in detail the mechanics of flexibility. Coralline algae are characterized by their calcified cell walls, which make them rigid. The earliest corallines were crusts composed of thin layers of cells adhering to the substratum, and their rigidity likely provided a defense against herbivore-induced disturbance (Johansen, 1981; Steneck, 1986; but see Padilla, 1985). However, approximately 100 million years ago some corallines evolved fronds that had 'joints' (genicula) spaced along their length (Johansen, 1981; Aguirre et al., 2010). The increased extensibility, increased compliance (that is, reduced stiffness) and high strength of the novel, uncalcified genicular tissue introduced flexibility into the previously rigid coralline body plan, allowing corallines to adopt an upright posture that offers several potential advantages. Flexible, erect fronds can avoid shading by uncalcified seaweeds (Johansen, 1981), can deter some grazers (Padilla, 1984) and may aid in spore dispersal (Johansen, 1981). Articulated corallines now thrive and successfully compete on wave-swept shores around the globe, often serving as ecosystem engineers whose densely packed fronds provide shelter to a wide variety of invertebrate animals.

The morphology, mechanical properties and chemical composition of genicular tissue vary considerably among coralline taxa (Janot and Martone, 2016), and an in-depth investigation of the interaction between these factors and overall frond flexibility is just beginning. Consequently, it is currently difficult to draw global conclusions about the structural underpinnings of genicular mechanics. However, the joints of *Calliarthron cheilosporioides* Manza, a representative articulated coralline found on the West Coast of North America (Fig. 1A,B), have been studied in detail, and *C. cheilosporioides* thus serves as a convenient species for an initial exploration of the morphological and chemical basis of coralline flexibility.

In some respects, *C. cheilosporioides*' genicular tissue is extraordinary: it is more extensible and much stronger than typical algal tissue (including other corallines; B. Hale, Macroalgal materials: foiling fracture and fatigue from fluid forces, PhD thesis, Stanford University, 2001; Martone, 2006, 2007; Janot and Martone, 2016) and it is virtually immune to failure by fatigue (Denny et al., 2013). However, in other respects, genicular tissue is rather ordinary. Its unusual mechanical properties are determined primarily by the characteristics of individual cell walls, which utilize a run-of-the-mill structural design: they are fiber-reinforced composites. Thus, *C. cheilosporioides*' genicula illustrate how modifying the structural and chemical components of a simple –

Hopkins Marine Station of Stanford University, Pacific Grove, CA 93950, USA.

*Author for correspondence (mwdenny@stanford.edu)

M.W.D., 0000-0003-0277-9022

Received 9 February 2016; Accepted 29 March 2016

Journal of Experimental Biology (2016) 219, 1833-1842 doi:10.1242/jeb.138859

List of symbols and abbreviations

a	major semiaxis of geniculum cross-section (m)
A	cross-sectional area of the breaking geniculum (m^2)
A_{gen}	cross-sectional area of a geniculum (m^2)
A_j	cross-sectional area of geniculum j (m^2)
A_{pl}	planform area of a frond (m^2)
b	minor semiaxis of geniculum cross-section (m)
C_D	drag coefficient (dimensionless)
D_{tan}	tangential compliance (Pa^{-1})
E_{tan}	tangential elastic modulus (Pa)
F	force (N)
F_D	drag (N)
H	hysteresis (dimensionless)
J	rotational second moment of area (m^{-4})
j	index identifying a particular geniculum
L	length of a geniculum (m)
L_j	length of geniculum j (m)
L_{tot}	total length of genicula in a sample (m)
M	moment (N m)
n	number of genicula in a sample
Re_f	frond Reynolds number (dimensionless)
t	time (s)
u	water velocity (m s^{-1})
u_{max}	maximum water velocity in a wave (m s^{-1})
α	average of $1/A_j$ in a sample (m^{-2})
γ	maximum shear strain (dimensionless)
$\Delta\varepsilon$	change in strain (dimensionless)
Δt	change in time (s)
ε	tensile strain (dimensionless)
θ	angle of the pendulum (rad)
σ	average stress in a wave cycle (Pa)
σ_i	instantaneous stress (Pa)
σ_{max}	maximum stress (Pa)
σ_n	nominal stress (Pa)
τ_{max}	maximum shear stress (Pa)
ϕ	angle of twist in a shear test (rad)

indeed, near-universal – cellular morphology can lead to functional innovation.

Although several aspects of *C. cheilosporioides*' genicular design have been explored, there are gaps in our understanding, and the disparate studies of the species' genicula have yet to be drawn together into a coherent story. This and our companion paper (Denny and King, 2016) are a first effort at such a synthesis. To gain a mechanistic understanding of *C. cheilosporioides*' genicular material, we used experimental data to fill in the missing pieces of information, and, in the companion paper, we propose a simple conceptual model that provides a mechanistic explanation for the behavior of this exceptional material.

First, some background from previous studies of *C. cheilosporioides*. Each geniculum is formed during growth as a single tier of frond cells decalcifies and extends tenfold along the frond's axis (Johansen, 1981). Mature genicular cells are approximately 500 µm long with each end firmly anchored in an adjacent intergeniculum, the calcified portion of the frond (Fig. 1C). These decalcified cells form the flexible joint. Genicular cells are hexagonal in cross-section, with an average diameter of ∼7 µm; there are 15,000 to 24,000 cells in each geniculum (Martone, 2007).

Cell walls form approximately 34% of the cross-sectional area of young cells, but this increases to 54% in older cells as secondary cell wall is laid down, a process not found in typical red algae (Martone, 2007). The cell walls are composed of randomly oriented cellulose fibers in a matrix gel of highly methylated, highly sulfated galactan (Tsekos et al., 1993; Martone et al., 2010; P. T. Martone, unpublished data). *Calliarthron cheilosporioides*' cell walls have a larger proportion of cellulose (15% of dry mass) than is typical of seaweeds, although this percentage is lower than that typical of terrestrial plants (30%) (Martone et al., 2010). Genicular cells are separated laterally by a middle lamina ∼1 µm thick. Middle laminae contain cellulose, but otherwise have an unknown chemical composition (P. T. Martone, Biomechanics of flexible joints in the seaweed *Calliarthron cheilosporioides*, PhD thesis, Stanford University, 2007; P. T. Martone, unpublished data).

Although genicula comprise only ∼15% of the length of a *C. cheilosporioides* frond, the frond's overall flexibility is comparable to that of uncalcified ('fleshy') seaweeds. This is possible only because genicular material is much more extensible than the tissues of typical macroalgae; *C. cheilosporioides*' joints can stretch to more than twice their length while most seaweeds can extend by only 25% to 50% (B. Hale, Macroalgal materials: foiling fracture and fatigue from fluid forces, PhD thesis, Stanford University, 2001; Martone and Denny, 2008a). The strength of *C. cheilosporioides*' cell-wall material is comparable to that of other algae, but because cell walls form an exceptionally large fraction of its cross-sectional area, *C. cheilosporioides*' genicular tissue is approximately four times stronger than typical algal tissue (B. Hale, Macroalgal materials: foiling fracture and fatigue from fluid forces, PhD thesis, Stanford University, 2001; Martone, 2006, 2007; P. T. Martone, unpublished data).

Although each genicular cell is firmly anchored to the adjacent intergenicula, lateral attachment among cells (via the middle lamina) is apparently weak (Martone and Denny, 2008b; Denny et al., 2013). As a result, if one cell breaks, it is difficult for the elastic energy stored in the broken cell to be transferred to adjacent cells. This inability to transfer the energy required for fracture makes it difficult for a crack to propagate, rendering the joint highly resistant to fatigue failure (Denny et al., 2013).

Calliarthron cheilosporioides' immunity to fatigue makes it possible for one to estimate the limit to the size of its fronds in the surf zone. Because joints do not weaken appreciably through repeated loadings, whether a frond will survive or not is determined by the largest force it encounters. (This is in contrast to fleshy red algae, in which the accumulated damage from small forces limits size; Mach, 2009; Mach et al., 2007, 2011.) Thus, from easily acquired records of maximum wave force (Denny and Wethey, 2001), one can accurately estimate the maximum size to which *C. cheilosporioides*' fronds can grow in a given wave environment (Martone and Denny, 2008a; Denny, 2016). Because *C. cheilosporioides* is a major competitor for space in the low intertidal zone, these estimates of maximum size can be valuable when considering the ecological consequences of a changing wave climate. If, as predicted, wave heights increase in the near future (IPCC, 2013), *C. cheilosporioides*' fronds will potentially be limited to a smaller size, reducing their ability to shade out competitors and substantially altering the niche they create for invertebrate animals.

In summary, our knowledge of the material mechanics of *C. cheilosporioides* allows us to connect mechanism across scales: from molecules to materials to whole organisms to community ecology. Despite this wealth of information, three important questions about *C. cheilosporioides*' joints must be addressed before a full synthesis is possible. (1) The extensibility, compliance and strength of genicular material have been measured as forces are applied over the course of 5–10 s. However, when loaded by wave-induced velocities, fronds are stretched in a fraction of a second. How does this high rate of deformation affect the extensibility,

Journal of Experimental Biology (2016) 219, 1833-1842 doi:10.1242/jeb.138859

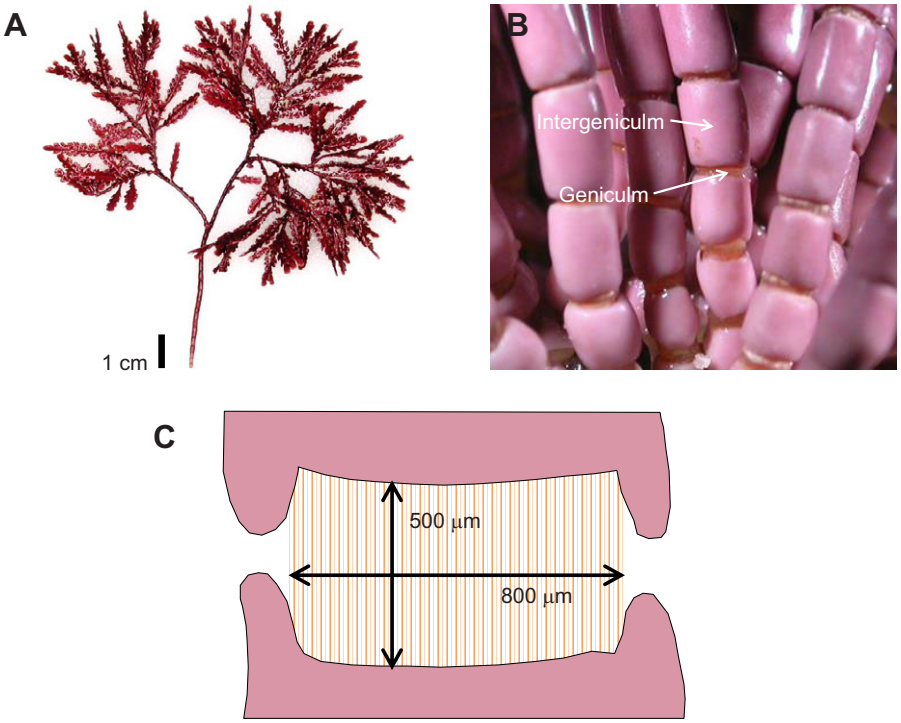

Fig. 1. The articulated coralline alga *Calliarthron cheilosporioides*. (A) An entire frond. Photo credit: Patrick Martone. (B) Fronds are composed of calcified intergenicula and the genicula ('joints') that connect them. Modified from Martone (2007). (C) A schematic drawing of a longitudinal section through a geniculum showing the single tier of genicular cells.

compliance and strength of *C. cheilosporioides*' joint material? (2) For many materials, application of repeated short-term stresses – or persistent long-term stress – causes the material to creep; that is, to accrue deformation through time. Given that *C. cheilosporioides* is repeatedly loaded by hydrodynamic forces at high tide and can be subjected to loads that persist for hours as fronds lie twisted and bent at low tide, does genicular material creep? If so, how much does a joint creep in its lifetime? Does creep affect joint flexibility? Can creep lead to failure? (3) Electron microscopy has revealed the fine structure of genicular cell walls (Martone, 2007; Martone et al., 2009; Janot and Martone, 2016; P. T. Martone, unpublished data), but it is currently unclear how this micro-scale architecture is tied to the tissue-scale mechanical properties of the material, and thereby to a frond's performance in nature. To what extent can we use a detailed description of genicular material properties to build an understanding of *C. cheilosporioides*' whole-frond mechanics, and thereby its success in an ecological context? We address questions 1 and 2 in this report; we address question 3 in the companion paper (Denny and King, 2016).

MATERIALS AND METHODS

Sample collection

Calliarthron cheilosporioides fronds were collected at Stanford University's Hopkins Marine Station (HMS) in Pacific Grove, CA, USA (36.622°N, 121.906°W), at the same lower intertidal site used in several previous studies (Martone, 2006, 2007; Martone and Denny, 2008a,b; Denny et al., 2013). Samples were held in chilled seawater (4°C) until used, usually within a day.

High strain rate tensile tests

Genicula were deformed at high rates using a ballistic pendulum (Fig. 2). The pendulum arm (66 cm long) was suspended from an axle held in place by ball bearings, and the angle of the pendulum relative to vertical (θ) was monitored by a rotary transducer (Model R30A, Schaevitz Engineering, Camden, NJ, USA). A rigid fork at the pendulum's free end served to apply a force to the test sample. Using marine epoxy (A-788 Splash Zone Compound, Kop-Coat Inc., Rockaway, NJ, USA), the sample (a length of basal frond containing approximately 10 genicula) was glued at its proximal end to the beam of a bespoke force transducer and at its distal end to an aluminium rod held in place by a linear bearing. A plastic (Delrin) disk attached to the rod at its free end served as the impact target for the tines of the pendulum's fork. To perform an experiment, the pendulum was pulled away from vertical and then released. As the pendulum swept down, the fork straddled the force transducer and sample before impacting the Delrin target. As the pendulum continued on its arc, the target was displaced, the sample was stretched, and the resulting force was monitored by the force transducer.

Strain gauges on the force transducer beam (wired as a full Wheatstone bridge) provided a voltage output proportional to the

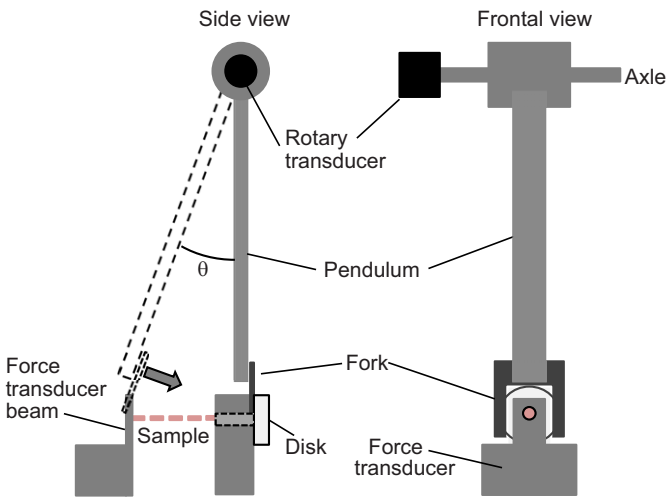

Fig. 2. A schematic diagram of the device used to measure tensile stress and strain in genicula at high strain rates. θ, angle of the pendulum.

Journal of Experimental Biology

Journal of Experimental Biology (2016) 219, 1833-1842 doi:10.1242/jeb.138859

tensile force acting on the test genicula. The force transducer was calibrated by hanging known weights from it, and it had a resonant frequency of 2885 Hz, sufficient to respond accurately to the forces applied by the swinging pendulum. Voltage signals from both the rotary and force transducers were digitized by an A/D converter (Model USB-6009, National Instruments, Austin, TX, USA) and recorded at 10 kHz, providing measures of force and tensile displacement through time. The sample was kept moist with seawater until tested, and tests were conducted at room temperature, 19–21°C.

The farther the pendulum was initially displaced, the higher its speed at impact, and the greater the rate at which the sample was strained. After each test, the length (L_j) and cross-sectional area (A_j) of each geniculum in the sample (j=1 to n, the total number of genicula in the test section) was measured using a dissecting microscope equipped with a vernier micrometer eyepiece. Area was calculated by measuring the major and minor diameters of the geniculum and approximating cross-sectional area as the area of an ellipse. For each $F(t)$ (the force recorded at time t), displacement of the sample's distal end [$\Delta L_{tot}(t)$] was calculated from the length of the pendulum and the difference in θ from that at the instant of impact.

For the geniculum that broke, nominal stress (σ_n) and strain (ε) were then calculated for each F–ΔL_{total} pair. Nominal stress is the applied force divided by the geniculum's unstressed cross-sectional area, A:

$$\sigma_n = \frac{F}{A}. \quad (1)$$

Strain in the broken geniculum (its change in length, ΔL, per its unstressed length, L) was calculated taking into account the variation in cross-sectional area among genicula (see Appendix):

$$\varepsilon = \frac{\Delta L_{tot}}{L_{tot} A \alpha}. \quad (2)$$

Here, α is the average of $1/A_j$ for all unglued genicula in the sample, and L_{tot} is the total unstressed length of all n genicula. Strain rate was estimated as the slope of a regression line fitted to ε as a function of time. Experimental strain rates varied from 207 to 825 s^{-1}.

The resulting stress–strain curves were non-linear, so the material's stiffness (its tangential elastic modulus $E_{tan}=d\sigma_n/d\varepsilon$) changes as a function of strain; that is, E_{tan} depends on how far a sample is extended. To calculate E_{tan} at a given strain, a third-order polynomial was fitted to the stress–strain data, and its first derivative (E_{tan}) was calculated at the desired strain. Only regressions with r^2>0.99 were used for these calculations (N=18). From these data, we calculated the material's compliance, $D_{tan}=1/E_{tan}$, at each of a series of strains. Although modulus is a more commonly used metric of material properties, compliance is a more intuitive metric of flexibility, and it is the standard for the creep tests described below (Aklonis et al., 1972).

Cyclic tensile stress–strain tests

The mechanical response of genicula to cyclic loading was measured using the tensometer employed by Martone (2006) and Martone and Denny (2008a), and the details of the apparatus can be found there. In short, a length of basal frond was held between two clamps, one supported by a force transducer and the other attached to the moveable head of the tensometer. The sample was extended at a rate of approximately 0.3 mm s^{-1} until a predetermined force was reached. The direction of the moving head was then reversed until stress reached zero. This cycle of extension/retraction was then repeated. Force was recorded digitally at 60 Hz with a resolution of 0.004 N. The force transducer was calibrated using known weights.

We measured the strain of individual genicula within the test section using a high-speed video camera (Fastcam 512PCI, Photron USA Inc., San Diego, CA, USA) with a resolution of approximately 10 µm. Small dots of black ink were scribed onto adjacent intergenicula in the middle of the test sample, which were videotaped at 60 Hz throughout the course of each test, synchronized with the force measurements. In each frame, the distance between dots on two adjacent intergenicula was calculated using image analysis software (Motion Tools v1.2.0, Photron USA Inc.), calibrated with an image of a stage micrometer, providing a measure of the change in length of the geniculum between the two intergenicula. After each test, the length and cross-sectional area of the imaged geniculum were measured as described above for the high strain rate tests. From these data, we calculated the strain of the geniculum and the corresponding nominal stress for each image in the test. The total energy per volume required to stretch the sample to the maximum strain in a given cycle was calculated as the area under the ascending leg of the stress–strain curve. The energy per volume stored during a cycle is the area under the descending leg, and the energy dissipated (again per volume) is the difference between the two. Hysteresis, H, for the cycle is the ratio of energy per volume dissipated to total energy per volume (Wainwright et al., 1976).

In a second set of tests using the same apparatus, the extension of the sample was halted, and force was recorded through time, allowing us to measure stress relaxation, the reduction in stress through time at constant strain. Subsequently, the strain imposed on the sample was reduced, the moving head was halted and force was again recorded through time, allowing us to measure stress recovery, the increase in stress through time at constant strain.

Shear stress/strain tests

Samples (collected as for the other experiments) were tested in shear using the apparatus shown in Fig. 3. Several intergenicula of a basal section of frond were glued at one end with Splash Zone Compound into a Delrin coupling. The coupling was then attached to a shaft supported by ball bearings, and the sample's free end was firmly clamped to a rigid support, leaving a single geniculum exposed. A moment was applied to the shaft by hanging a length of fine-link brass chain (0.294 g cm^{-1}) from a capstan (1.25 cm in radius) on the shaft. The length of the hanging chain was adjusted by raising or lowering a platform beneath the chain; lowering the platform allowed more weight to hang from the capstan, applying a larger

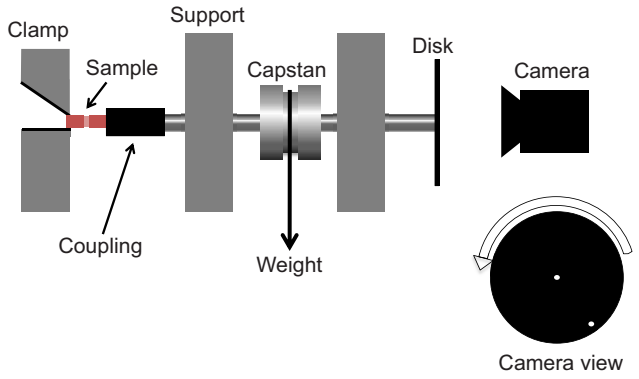

Fig. 3. A schematic diagram of the device used to measure shear stress and strain in genicula.

moment (3.67×10^{-5} N m cm^{-1}). The platform was lowered and raised in 0.5 cm increments. Rotation of the geniculum was measured for each increment of moment using a video camera (c525 HD Webcam, Logitech Inc., Fremont, CA, USA) to optically track the rotation of a white spot on a black disk affixed to the free end of the shaft. The angle of the spot relative to the disk's center was analyzed using the Image Processing Toolbox in MATLAB (MathWorks, Natick, MA, USA); angles were accurate to 0.0095 rad with a precision of 0.0013 rad. During the test, the sample was kept wet and at 19°C by a continuous seawater drip from a peristaltic pump.

For an object in torsion – such as the geniculum in this experiment – shear strain (and therefore shear stress) increases with radial distance from the center of twist. For these tests, we used maximum shear stress as our metric of applied force. Maximum shear stress in the sample was calculated as:

$$\tau_{max} = \frac{Ma}{J}, \quad (3)$$

where M is the applied moment (the force of the chain's weight multiplied by the radius of the capstan), a is the major semiaxis of the geniculum's cross-section and J is the rotational second moment of area of the geniculum's elliptical cross-section (Timoshenko and Gere, 1972):

$$J = \frac{\pi ab}{4}(a^2 + b^2). \quad (4)$$

Here, b is the minor semiaxis of the cross-section.

Maximum shear strain, γ, was calculated from the geniculum's length, L, major semiaxis, a, and the angle, ϕ, through which the geniculum was twisted:

$$\gamma = \frac{\phi a}{L}. \quad (5)$$

The sample's dimensions were measured after the test was completed. Hysteresis was calculated as for the experiments in tension.

Creep

Tensile creep

Tensile creep tests were performed coincidentally with the fatigue tests conducted by Denny et al. (2013), and details of the apparatus can be found there. In short, a test sample (8–11 genicula) was excised from a basal section of a frond, and the cross-sectional areas of the end genicula were measured as described above. The average of these areas was used as an estimate of the area of genicula in the rest of the sample. The sample was then glued in place between a force transducer and an oscillating beam, leaving 4–7 genicula exposed. The motion of the beam sinusoidally strained the sample at 10.1 Hz, with force varying from 0 to that necessary to apply a peak stress, σ_{max}, a set fraction of *C. cheilosporioides*' nominal tensile breaking stress. As the genicula crept, becoming longer and thinner, the amplitude of the beam's oscillation was adjusted by computer to maintain constant force per cross-sectional area. However, as the genicula lengthened, the oscillation of the beam caused the sample to become slack when the beam moved closest to the force transducer. As a consequence, to maintain the sinusoidal pattern of stress, it was necessary to gradually move the force transducer away from the oscillating beam, an adjustment effected by a computer-controlled stepping motor attached to a fine-pitched screw. The distance moved by the transducer relative to the total length of the genicula in the sample is a measure of the strain accruing through time resulting from the cyclical stress, making it a measure of tensile creep. Because the sample was loaded sinusoidally, the average stress in each cycle, σ, was equal to half the peak stress, σ_{max}, and we treat these data as an approximation of how a geniculum would creep under a constant stress equal to the average. (This is equivalent to assuming that creep is due to a Newtonian viscous process, in which strain rate is proportional to stress; Aklonis et al., 1972.)

Strain was recorded every 20 s for the first 5300 cycles and every 60 s thereafter until the sample broke from fatigue. Samples were immersed in seawater at 12–13°C during testing, and the seawater was changed daily. We obtained data for 21 samples.

After the sample broke, the cross-sectional area of the failed geniculum was measured, allowing us to calculate the actual applied stress. Knowing stress and strain, we could then calculate the sample's compliance as a function of time:

$$D(t) = \frac{\varepsilon(t)}{\sigma}. \quad (6)$$

Shear creep

Samples (collected as for other tests) were tested in shear using the same apparatus as for shear stress–strain measurements (Fig. 3). Instead of the chain, a 10 g mass was hung from the capstan by a fine thread, applying a moment of 1.23×10^{-3} N m. An image of the disk was acquired every second for the first 60 s of the experiment, and every 30 s thereafter for 6–12 h. Shear stress and maximum shear strain were calculated as before and used to calculate compliance, $D(t)$. The sample was kept moist and at a constant 19°C with a seawater drip.

The tensile and shear creep measurements complement each other: to accommodate computer control of strain in the tensile-testing apparatus, creep could not be measured during the initial cycles required to adjust the apparatus to apply a constant stress; testing genicula in shear allowed us to characterize creep over the initial period missed in the tensile tests.

Estimating lifetime creep

We used data from the tensile creep tests to estimate the creep a basal geniculum would accumulate during the lifetime of a frond in the surf zone. We first fitted a curve to a sample's tensile compliance as a function of time (a representative example is shown in Fig. 4A). The derivative of that curve is our estimate of dD/dt, the temporal rate of change of compliance. However, for each measured value of dD/dt, we know the corresponding strain, which allows us to plot dD/dt as a function of strain rather than time (Fig. 4B). Because $D=\varepsilon/\sigma$, $dD/dt=d(\varepsilon/\sigma)/dt$, so, for a constant average stress:

$$\left(\frac{dD}{dt}\right)_\varepsilon = \frac{1}{\sigma}\left(\frac{d\varepsilon}{dt}\right)_\varepsilon. \quad (7)$$

(Here, the subscript ε denotes that the factor in parentheses is evaluated at a particular strain.) Thus, for a given strain and stress, Fig. 4B allows us to estimate how much a sample's compliance, and hence its strain, changes in time dt.

Our next task was to describe how stress on a basal geniculum varies through time as waves impinge on the shore. Drag, F_D, is applied to a frond by the velocity of the water, u (Denny, 1988, 2016; Vogel, 1994), such that at a given time t:

$$F_D(t) = \frac{1}{2}\rho u^2(t) A_{pl} C_D, \quad (8)$$

Journal of Experimental Biology (2016) 219, 1833-1842 doi:10.1242/jeb.138859

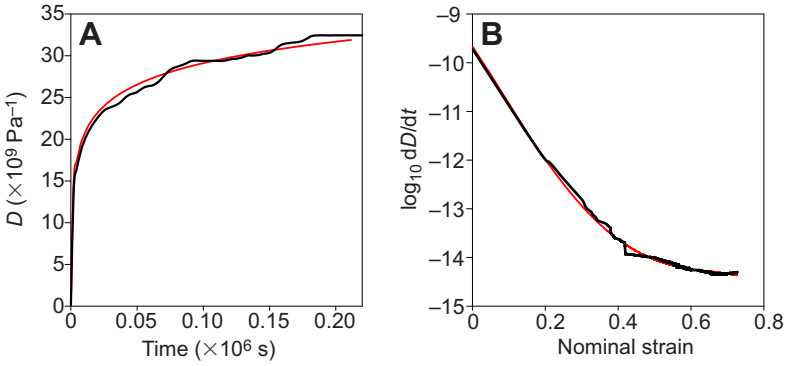

Fig. 4. Creep and compliance in *C. cheilosporioides*' genicula. (A) A representative record of tensile creep. The red line is a logarithmic fit to the data: y=3.703ln(x)+37.648 (r^2=0.986), where x is time (×10^6 s) and y is compliance (D, ×10^9 Pa^{-1}). (B) Compliance expressed as a function of strain rather than time. The red line is a polynomial fit to the data: y=−27.813x^4+40.85x^3−8.215x^2−11.372x−9.6624 (r^2=0.981).

where ρ is the density of seawater (1025 kg m^{-3}), A_{pl} is the frond's planform area (approximately half its wetted area) and C_D is the frond's drag coefficient (Martone and Denny, 2008a):

$$\log_{10}C_D = -2.06 + 223.24(\log_{10}Re_f)^{-3.58}. \quad (9)$$

Here, Re_f is the frond Reynolds number:

$$Re_f = \frac{\rho u\sqrt{A_{pl}}}{\mu}, \quad (10)$$

where μ is the viscosity of seawater (1.24×10^{-3} Pa s) at 15°C (a representative temperature at HMS; Denny, 1993). In short, if we know u and A_{pl}, we can calculate F_D (Fig. 5A). Dividing by the cross-sectional area of a basal geniculum, A_{gen}, then gives us instantaneous stress, σ_i, as a function of water velocity, u, during the passage of a wave:

$$\sigma_i(t) = \frac{\rho u^2(t)A_{pl}C_D}{2A_{gen}}. \quad (11)$$

We next model the time course of velocity in each wave after Hata (T. Hata, Measuring and recreating hydrodynamic environments at biologically relevant scales, PhD thesis, Stanford University, 2015), based on measurements taken at the site where *C. cheilosporioides* was collected (Fig. 5B). Waves are assumed to have a period of 10 s (typical of the shore at HMS). In the initial 4 s after a wave arrives at the shore:

$$u(t,u_{max}) = 1 - \left\{\left|\sin\left[\pi\left(\frac{t-2}{4}\right)\right]\right|\right\}^{1/3}u_{max}. \quad (12)$$

Here, t is time (s), u is instantaneous velocity (m s^{-1}) and u_{max} is the maximum velocity in the wave. In the subsequent 6 s:

$$u(t,u_{max}) = 1910\left(\frac{t-4}{6}\right)^9\left[1-\left(\frac{t-4}{6}\right)\right]^{4.5}u_{max}. \quad (13)$$

Knowing u through the course of a wave, we can calculate instantaneous stress through the wave (Eqn 11), and, for a given u_{max}, we can integrate σ_i through time Δt to calculate average stress, σ:

$$\sigma = \frac{1}{\Delta t}\int_0^{\Delta t}\sigma_i(t,u_{max})\mathrm{d}t. \quad (14)$$

Multiplying both sides of this equation by Δt adjusts the expression to the form in which it will be used in the next calculation (Fig. 5C):

$$\sigma\Delta t = \int_0^{\Delta t}\sigma_i(t,u_{max})\mathrm{d}t. \quad (15)$$

For our calculations, Δt is 10 s, the wave period. This calculation, along with the information in Fig. 4B, allows us to calculate the increment in strain accruing from each wave. Estimating dD/dt (Eqn 7) as $\Delta D/\Delta t$:

$$\left(\frac{\Delta D}{\Delta t}\right)_\varepsilon \sigma\Delta t = \frac{1}{\sigma}\left(\frac{\Delta\varepsilon}{\Delta t}\right)_\varepsilon \sigma\Delta t = (\Delta\varepsilon)_\varepsilon. \quad (16)$$

In summary, we use frond and genicular areas to calculate the increment in strain resulting when a wave with maximum velocity u_{max} and a period of 10 s is imposed on a geniculum with pre-existing strain ε.

Using this mathematical framework, we then draw from the distribution of u_{max} recorded at our site by Mach et al. (2011) to sum these strain increments through time beginning at ε=0. From a random selection of 86,400 u_{max} values recorded by Mach et al. (2011), we draw the u_{max} of one wave at random and calculate Δε, the increase in strain after one wave (10 s). We then choose another u_{max} at random, calculate a new Δε, and add it to the previous strain to give ε after 20 s. This procedure is then iterated until t=1.892×10^8 s (1.892×10^7 waves), the estimated 6 year maximum lifetime of *C. cheilosporioides* (Martone, 2010). Because dD/dt is a function of ε (Fig. 4B), cumulative strain depends on the order in which stresses are applied. Therefore, to characterize lifetime creep, we repeated this process 10 times and took the average.

RESULTS

High strain rate tensile tests

A representative stress–strain curve is shown in Fig. 6A. Averaged across samples, tensile compliance D_{tan} decreases gradually with increasing strain (Fig. 6B). Breaking stress is not significantly correlated with strain rate (P=0.290) for the strain rates involved in these tests (207 to 825 s^{-1}). Similarly, although compliance varies with strain, it is independent of strain rate (P=0.338, 0.186, 0.136, 0.094 and 0.058 at strains of 0.1, 0.2, 0.3, 0.4 and 0.5, respectively). By contrast, breaking strain is positively correlated with strain rate (Fig. 6C; P<0.001, r^2=0.478).

Cyclic stress–strain

Tension

Representative tensile cyclic stress–strain data are shown in Fig. 7A, with the first cycle shown in red and the second cycle in black. In the first cycle, an average of 42.4±4.1% (±s.e.m.) of the strain energy required to extend the sample in tension is lost to viscous processes upon retraction (that is, its hysteresis, H=0.424). At least part of the energy lost can be attributed to plastic strain (average plastic strain=0.018±0.007, 13.1±3.6% of the cycle's maximum strain). After an extension/retraction cycle, subsequent cycles to higher strains

Journal of Experimental Biology (2016) 219, 1833-1842 doi:10.1242/jeb.138859

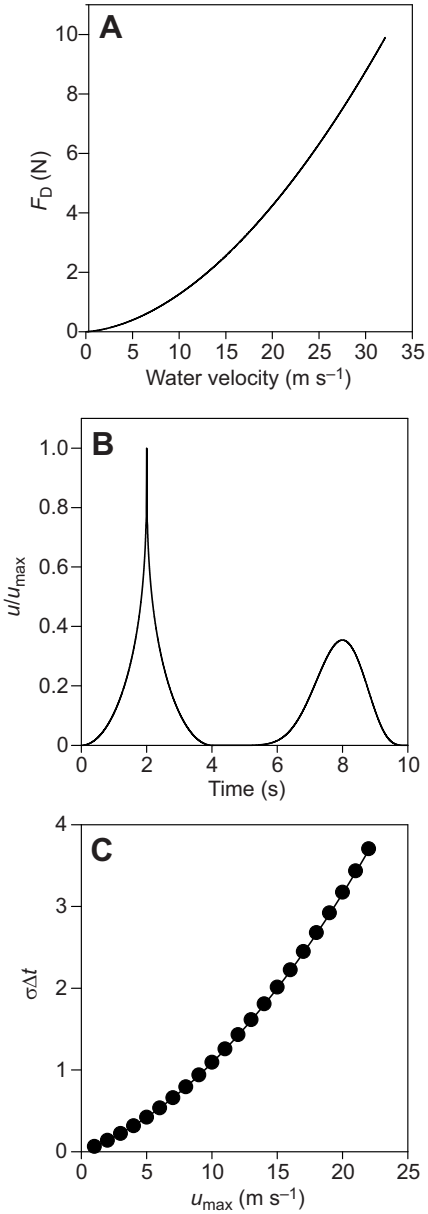

Fig. 5. Components of the calculation of lifetime creep. (A) Drag, F_D, as a function of water velocity for a frond with a planform area of 20 cm^2 (Eqn 8). (B) The average time course of relative water velocity (u/u_{max}) during a wave with a period of 10 s (Eqns 12 and 13). (C) The stress (σ)–time increment (Δt=10 s) accrued by a frond with planform area 20 cm^2 as a function of the maximum velocity (u_{max}) in a wave (Eqn 15).

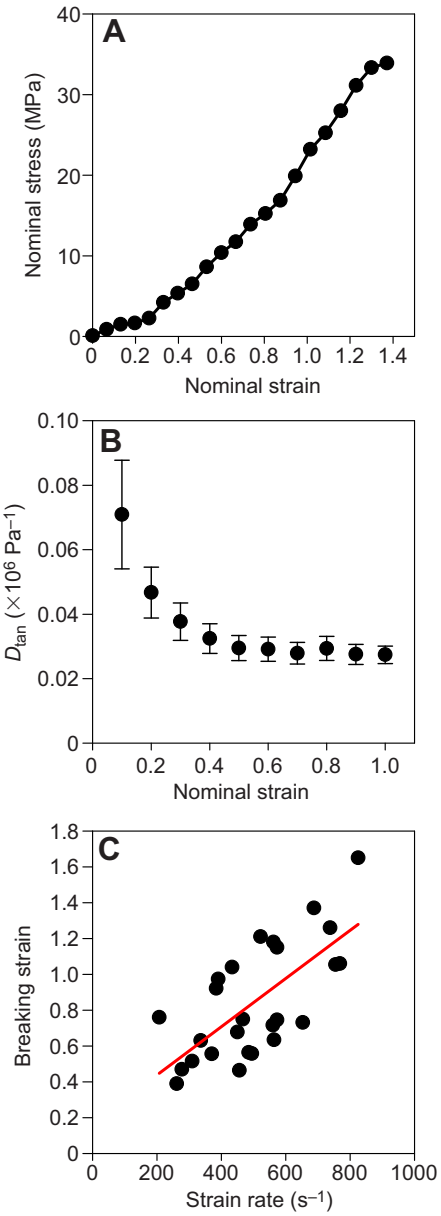

Fig. 6. Results of the high strain rate tensile tests. (A) A representative stress–strain curve. The strain rate in this test was 688 s^{-1}. (B) Average compliance (D_{tan}, tangential compliance) as a function of strain; the error bars are s.e.m. (C) Breaking strain is positively correlated with strain rate.

have a stress–strain curve in extension that takes up where the previous cycle left off (arrow in Fig. 7A). Hysteresis is lower in the second and subsequent cycles (H=0.306±0.025 on average for the second cycle), and plastic strain is reduced (on average, only 2.2±1.5% of the additional strain in the second cycle is not recovered).

When a stress cycle is interrupted during extension, stress in the sample decreases through time (stress relaxation; a representative test is shown in Fig. 7B). By contrast, when a cycle is interrupted during decreasing stress, stress in the sample subsequently increases through time (stress recovery).

Shear

Representative torsional cyclic stress–strain data are shown in Fig. 8. Genicula in shear have a higher hysteresis than in tension (Student's t-test, P<<0.001), due at least in part to greater plastic deformation. In the first cycle, on average 81.2±3.9% of strain energy required to extend the sample is dissipated upon retraction (compared with 42% for tension), with average plastic strain of 0.17±0.035, 50% of the cycle's maximum strain (compared with 13% for tension). Hysteresis is lower in the second and subsequent cycles (58.2±2.6% on average for the second cycle), and plastic strain is reduced (on average, 8.9±3.9% of the additional strain in the second cycle is not recovered). In subsequent cycles, hysteresis and plastic strain remain higher than for samples loaded in tension.

Creep

Tension

Average tensile compliance increases continuously through time with no hint of a plateau (Fig. 9A).

Journal of Experimental Biology (2016) 219, 1833-1842 doi:10.1242/jeb.138859

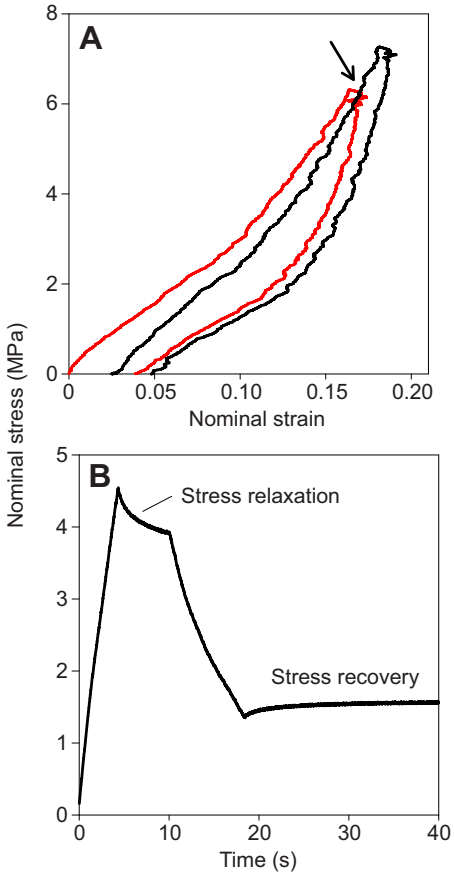

Fig. 7. Results from the cyclic tensile tests. (A) Representative results from the initial two cycles of strain. The red line is the first cycle, the black line the second cycle. Note that the stress due to incremental strain in the second cycle takes up where the first cycle left off (arrow). (B) A test showing stress relaxation when the moving head is stopped while stress is increasing, and stress recovery when the head is subsequently stopped as stress decreases.

Shear

The temporal course of creep in shear is similar to that in tension: compliance increases continuously through time (Fig. 9B). Note the rapid increase in compliance in shear at times shorter than those measured in tension. Compliance in shear is approximately 30 times higher than that in tension.

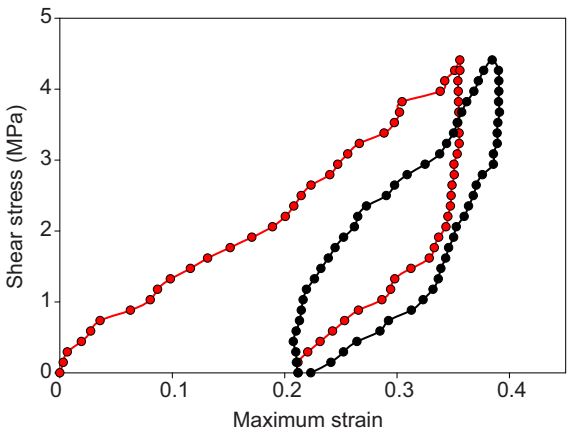

Fig. 8. Representative results from the cyclic shear tests. The red line is the initial cycle, the black line the second cycle.

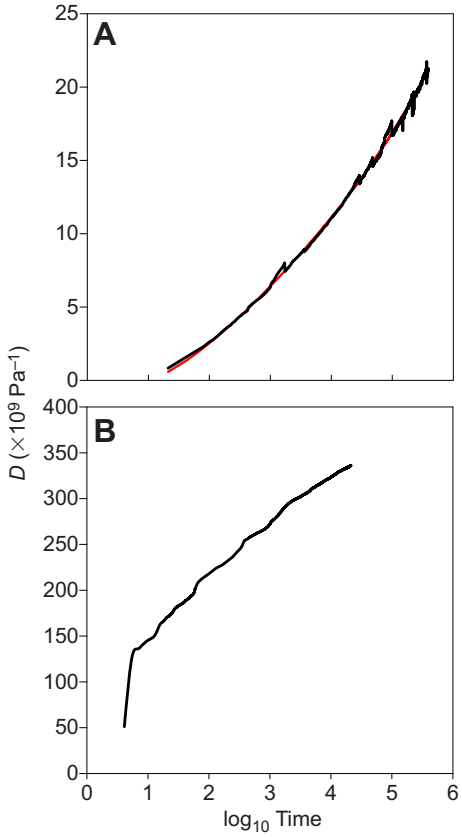

Fig. 9. Average creep behavior of genicular material in tension and shear. (A) In tension, different samples survived for different periods, leading to the ragged jumps in compliance (*D*) as the number of tests included in the average decreased as time increased. Red line is a fit to the data. (B) Creep in shear. Time was measured in s.

Lifetime accumulated creep

Assuming that waves arrive every 10 s for a 6 year lifetime (18.9 million stress cycles), the basal geniculum of a large frond (A_{pl}=20 cm^2) accumulates a strain of at most 0.357 in response to a realistic distribution of wave impacts (Fig. 10). Exposure to 100 million waves (31.7 years) would impose a strain only slightly larger, 0.464. These are likely overestimates in that they assume that waves arrive continuously; in reality, wave forces are not applied during extreme low tides. Creep estimates varied among our 10 replicate calculations, but this variation was substantial only when a small number of wave cycles were taken into account: the coefficient of variation (s.d./mean) was 0.15 for strain after 100 waves, 0.006 for strain after 10^4 waves, 4.6×10^{-5} for a 6 year estimate and 3.4×10^{-5} for 10^8 stress cycles.

DISCUSSION

Five aspects of the genicula's material properties are key to its function in *C. cheilosporioides*' joints: the material must be (1) sufficiently strong to withstand the stress imposed as joints twist, bend and extend; it must be (2) sufficiently compliant and (3) sufficiently extensible to provide the flexibility fronds need to cope with individual hydrodynamic insults, and it must resist both (4) fatigue and (5) creep to ensure that fronds can survive a lifetime of accumulated stress and strain. *Calliarthron cheilosporioides*' genicula fulfill these requirements through an unusual combination of properties.

On the one hand, genicula behave as one might expect from a solid. For an ideal solid, strength and compliance are independent of strain

Journal of Experimental Biology

Journal of Experimental Biology (2016) 219, 1833-1842 doi:10.1242/jeb.138859

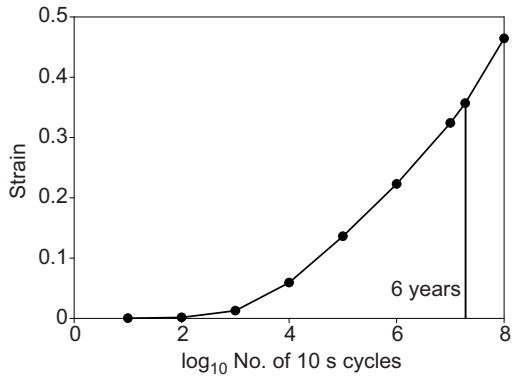

Fig. 10. Predicted accumulated strain as a function of the number of stress–strain cycles. The number of cycles was calculated using a wave period Δt of 10 s.

rate. In our tests, breaking stress was independent of strain rate across a wide range of rates, and the compliance measured at a strain rate of several hundred per second is comparable to that measured by Martone (P. T. Martone, Biomechanics of flexible joints in the seaweed *Calliarthron cheilosporioides*, PhD thesis, Stanford University, 2007) at a rate of 0.2 s^{-1} (4.7×10^{-8} Pa^{-1} versus 3.7×10^{-8} Pa^{-1}, respectively, at ε=0.2; 2.91×10^{-8} Pa^{-1} versus 2.17×10^{-8} Pa^{-1} at ε=0.5). The strain-rate independence of compliance may be advantageous. A mathematical model of *C. cheilosporioides*' genicula (Martone and Denny, 2008b) suggests that if compliance were to decrease with increasing strain rate (as it would in a typical viscoelastic material), stress in a basal joint would increase substantially, amplifying the likelihood of failure. However, because compliance is functionally independent of strain rate, genicula have the same flexibility across a wide range of loading regimes, a potential advantage in flow as unpredictable as that of breaking waves. Furthermore, the extensibility of genicular material actually increases with increasing strain rate (Fig. 6C). While this increase in breaking strain is not typical of elastic materials (indeed, it is, to our knowledge, unique among biological materials), it provides the seaweed with an extra bit of flexibility when responding to wave impact, which potentially bolsters its chance of survival.

These advantageous attributes of the material's elasticity are augmented by its viscous nature. Although viscosity has no apparent effect on compliance at strain rates from 0.2 to 825, it can nonetheless potentially enhance joint function. The dissipation of strain energy in cyclic loading – due in part to plastic deformation (Fig. 7A) – reduces the stored energy available to extend any flaws in the material, and thereby has the potential to reduce the risk of fatigue failure (Denny et al., 2013). However, when subjected to constant or repeated loads, genicula creep (Fig. 9) and one might suppose that this accumulated strain could threaten the joints. But Martone and Denny (2008b) have shown that an increase in genicular length increases a basal joint's flexibility, and, for strains less than 50%, the increase in flexibility is accompanied by negligible change in tensile stress. We estimate that basal genicula creep by maximally 36% over a 6 year lifetime (Fig. 10), so the creep they incur has the potential to increase flexibility without appreciably increasing stress. Another, closely related coralline alga (*Calliarthron tuberculosum*) living in British Columbia has a longer life span (11 years; Fisher and Martone, 2014), suggesting that at a different site, *C. cheilosporioides* might live longer and therefore accrue more strain. But even if it lived for more than 30 years, creep would still be less than 50%, and thus would not amplify tensile stress.

Conclusions

Measurements of how genicula respond to rapid strains, cyclical loading and the imposition of constant stress reveal the material's viscoelastic nature. In each case, the properties of the genicular material appear advantageous to the joints' function of providing flexibility to otherwise rigid fronds. In addition, the results described here in the context of genicular function can also be used in combination with previous findings to understand how the material properties of *C. cheilosporioides*' genicula can be explained by the microscale structure of genicular cell walls. We address this task in the companion paper (Denny and King, 2016).

It remains to be seen whether the mechanical adaptations apparent in *C. cheilosporioides*' joints are present in the genicula of other articulated corallines, many of which have arrived at their present morphology through different evolutionary and developmental pathways (Johansen, 1981; Janot and Martone, 2016).

Appendix

Because cross-sectional area varied between genicula in the test sample, stress (and therefore strain) varied among joints. To calculate the nominal strain (change in length, ΔL, per unstressed length, L) in a particular geniculum corresponding to a particular applied force, F, we assumed that tensile modulus (E, stress divided by strain) is constant for all genicula in the sample. Thus:

$$E = \frac{\sigma}{\varepsilon} = \frac{F/A_j}{\Delta L_j/L_j}. \quad \text{(A1)}$$

Here, j=1, 2, …, n denotes the individual geniculum, and n is the total number of genicula in the test portion of the sample. Rearranging, we find that:

$$\Delta L_j = \frac{FL_j}{EA_j}. \quad \text{(A2)}$$

Summing across all genicula:

$$\Delta L_{\text{tot}} = \sum_{j=1}^{n} \Delta L_j = \frac{F}{E}\sum_{j=1}^{n} \frac{L_j}{A_j}. \quad \text{(A3)}$$

Noting that:

$$\sum_{j=1}^{n} \frac{L_j}{A_j} = n\left\langle \frac{L_j}{A_j} \right\rangle, \quad \text{(A4)}$$

where the brackets denote the average,

$$E = \frac{Fn\left\langle \frac{L_j}{A_j} \right\rangle}{\Delta L_{\text{tot}}}. \quad \text{(A5)}$$

For *C. cheilosporioides*, L is relatively consistent among genicula within a frond, so:

$$E \approx \frac{Fn\langle L\rangle\left\langle \frac{1}{A_j} \right\rangle}{\Delta L_{\text{tot}}} = \frac{FL_{\text{tot}}\left\langle \frac{1}{A_j} \right\rangle}{\Delta L_{\text{tot}}}. \quad \text{(A6)}$$

Because $E=\sigma/\varepsilon$:

$$\varepsilon_j = \frac{F/A_j}{E}. \quad \text{(A7)}$$

Combining Eqns A6 and A7, we conclude that:

$$\varepsilon_j = \frac{\Delta L_{\text{tot}}}{L_{\text{tot}}A_j\left\langle \frac{1}{A_j} \right\rangle}. \quad \text{(A8)}$$

For nomenclatural simplicity, let $\left\langle \frac{1}{A_j} \right\rangle = \alpha$. Thus, strain ε in the broken geniculum, which has cross-sectional area A, is:

$$\varepsilon = \frac{\Delta L_{\text{tot}}}{L_{\text{tot}} A \alpha}. \quad \text{(A9)}$$

Acknowledgements
We thank Sarah Tepler for assistance with the high strain rate experiments, Tad Finkler for designing the software for the tensile creep apparatus, and Patrick Martone for advice and insight regarding all aspects of *C. cheilosporioides*' mechanics and natural history.

Competing interests
The authors declare no competing or financial interests.

Author contributions
F.A.K. designed the torsional apparatus, performed and analyzed the shear experiments, and contributed to the writing of the manuscript. M.W.D. designed the other apparatus, performed and analyzed the other experiments and was primarily responsible for writing the manuscript.

Funding
This work was funded by National Science Foundation grants IOS-0641068 and IOS-1130095 to M.W.D., for which we are grateful.

References

Aguirre, J., Perfectti, F. and Braga, J. C. (2010). Integrating phylogeny, molecular clocks, and the fossil record in the evolution of coralline algae (Corallinales and Sporolithales, Rhodophyta). *Paleobiology* **36**, 519-533.
Aklonis, J. J., MacKnight, W. J. and Shen, M. (1972). *Introduction to Polymer Viscoelasticity.* New York: Wiley-Interscience.
Boller, M. L. and Carrington, E. (2006). The hydrodynamic effects of shape and size change during reconfiguration of a flexible macroalga. *J. Exp. Biol.* **209**, 1894-1903.
Denny, M. W. (1988). *Biology and the Mechanics of the Wave-Swept Environment*. Princeton, New Jersey: Princeton University Press.
Denny, M. W. (1993). *Air & Water: The Physics of Life's Media*. Princeton, New Jersey: Princeton University Press.
Denny, M. W. (2016). *Ecological Mechanics: Principles of Life's Physical Interactions*. Princeton, New Jersey: Princeton University Press.
Denny, M. W. and Gaylord, B. (2002). The mechanics of wave-swept algae. *J. Exp. Biol.* **205**, 1355-1362.
Denny, M. W. and King, F. A. (2016). The extraordinary joint material of an articulated coralline alga. II. Modeling the structural basis of its mechanical properties. *J. Exp. Biol.* **219**, 1843-1850.
Denny, M. W. and Wethey, D. (2001). Physical processes that generate patterns in marine communities. In *Marine Community Ecology* (ed. M. D. Bertness, S. D. Gaines and M. E. Hay), pp. 3-38. Sunderland, Massachusetts: Sinauer Associates, Inc.
Denny, M. W., Miller, L. P., Stokes, M. D., Hunt, L. J. H. and Helmuth, B. S. T. (2003). Extreme water velocities: Topographical amplification of wave-induced flow in the surf zone of rocky shores. *Limnol. Oceanogr.* **48**, 1-8.
Denny, M., Mach, K., Tepler, S. and Martone, P. (2013). Indefatigable: an erect coralline alga is highly resistant to fatigue. *J. Exp. Biol.* **216**, 3772-3780.
Fisher, K. and Martone, P. T. (2014). Field study of growth and calcification rates of three species of articulated coralline algae in British Columbia, Canada. *Biol. Bull.* **226**, 121-130.
Gaylord, B. (1999). Detailing agents of physical disturbance: wave-induced velocities and accelerations on a rocky shore. *J. Exp. Mar. Biol. Ecol.* **239**, 85-124.
Harder, D. L., Speck, O., Hurd, C. L. and Speck, T. (2004). Reconfiguration as a prerequisite for survival in highly unstable flow-dominated habitats. *J. Plant Growth Regul.* **23**, 98-107.
IPCC (2013). *Climate Change 2013: The Physical Science Basis. Contribution of Working Group 1 to the Fifth Assessment Report of the Intergovernmental Panel on Climate Change* (ed. T. F. Stocker, D. Qin, G.-K. Plattner, M. Tignor, S. K. Allen, J. Boschung, A. Nauels, Y. Xia, V. Bex and P. M. Midgely). Cambridge, UK: Cambridge University Press.
Janot, K. and Martone, P. T. (2016). Convergence of joint mechanics in independently evolving, articulated coralline algae. *J. Exp. Biol.* **219**, 383-391.
Johansen, H. W. (1981). *Coralline Algae, a First Synthesis.* Boca Raton, Florida: CRC Press.
Koehl, M. A. R. (1984). How do benthic organisms withstand moving water? *Am. Zool.* **24**, 57-70.
Koehl, M. A. R. (1986). Seaweeds in moving water: form and mechanical function. In *On the Economy of Plant Form and Function* (ed. T. J. Givnish), pp. 603-634. Cambridge, UK: Cambridge University Press.
Mach, K. J. (2009). Mechanical and biological consequences of repetitive loading: crack initiation and fatigue failure in the red macroalga *Mazzaella*. *J. Exp. Biol.* **212**, 961-976.
Mach, K. J., Hale, B. B., Denny, M. W. and Nelson, D. V. (2007). Death by small forces: a fracture and fatigue analysis of wave-swept macroalgae. *J. Exp. Biol.* **210**, 2231-2243.
Mach, K. J., Tepler, S. K., Staaf, A. V., Bohnhoff, J. C. and Denny, M. W. (2011). Failure by fatigue in the field: a model of fatigue breakage for the macroalga *Mazzaella*, with validation. *J. Exp. Biol.* **214**, 1571-1585.
Martone, P. T. (2006). Size, strength and allometry of joints in the articulated coralline *Calliarthron*. *J. Exp. Biol.* **209**, 1678-1689.
Martone, P. T. (2007). Kelp versus coralline: cellular basis for mechanical strength in the wave-swept seaweed *Calliarthron* (Corallinaceae, Rhodophyta). *J. Phycol.* **43**, 882-891.
Martone, P. T. (2010). Quantifying growth and calcium carbonate deposition of *Calliarthron cheilosporioides* (Corallinales, Rhodophyta) in the field using a persistent vital stain. *J. Phycol.* **46**, 13-17.
Martone, P. T. and Denny, M. W. (2008a). To break a coralline: mechanical constraints on the size and survival of a wave-swept seaweed. *J. Exp. Biol.* **211**, 3433-3441.
Martone, P. T. and Denny, M. W. (2008b). To bend a coralline: effect of joint morphology on flexibility and stress amplification in an articulated calcified seaweed. *J. Exp. Biol.* **211**, 3421-3432.
Martone, P. T., Estevez, J. M., Lu, F., Ruel, K., Denny, M. W., Somerville, C. and Ralph, J. (2009). Discovery of lignin in seaweed reveals convergent evolution of cell-wall architecture. *Curr. Biol.* **19**, 169-175.
Martone, P. T., Navarro, D., Stortz, C. and Estevez, J. M. (2010). Differences in polysaccharide structure between calcified and uncalcified segments in the coralline *Calliarthron cheilosporioides* (Corallinales, Rhodophyta). *J. Phycol.* **46**, 507-515.
Martone, P. T., Kost, L. and Boller, M. (2012). Drag reduction in wave-swept macroalgae: alternative strategies and new predictions. *Am. J. Bot.* **99**, 806-815.
Padilla, D. K. (1984). The importance of form: differences in competitive ability, resistance to consumers and environmental stress in an assemblage of coralline algae. *J. Exp. Mar. Biol. Ecol.* **79**, 105-127.
Padilla, D. K. (1985). Structural resistance of algae to herbivores: a biomechanical approach. *Mar. Biol.* **90**, 103-109.
Steneck, R. S. (1986). The ecology of coralline algal crusts: convergent patterns and adaptive strategies. *Ann. Rev. Ecol. Syst.* **17**, 273-303.
Timoshenko, S. P. and Gere, J. M. (1972). *Mechanics of Materials*. New York: Van Nostrand.
Tsekos, I., Reiss, H.-D. and Schnepf, E. (1993). Cell-wall structure and supramolecular organization of the plasma membrane of marine red algae visualized by freeze-fracture. *Acta Bot. Neerl.* **42**, 119-132.
Vogel, S. (1994). *Life in Moving Fluids*. Princeton, New Jersey: Princeton University Press.
Wainwright, S. A., Biggs, W. D., Currey, J. D. and Gosline, J. M. (1976). *Mechanical Design in Organisms.* Princeton, New Jersey: Princeton University Press.

Journal of Experimental Biology